ISSN 2347-4289

Study Of Thermally Induced Residual Stresses For Stainless Steel Grade Using GMAW Process

M. Chougule, M. Unhale, A. Walunj, S. Chavhan, S. Somase.

Sinhgad Institute of technology, Lonavala, Pune, Maharashtra, India, 410401.
Email: amoldwalunj@gmail.com

ABSTRACT: Welding is a reliable and effective metal fabrication process which is widely used in industries. High heating at a one location during welding and further rapid cooling generates residual stress and distortion in the weld and base metal. In last few decades various research efforts have been directed towards the control of welding process parameter aiming at reducing residual stress and distortion. Residual stress distribution and distortion in welded plate are strongly affected by many parameters like structural, material and welding parameters. Such welding failure can be minimized by controlling the weld heat input. The distribution of the temperature in weld joint of AISI202 grade high strength steel was investigated by Finite Element Method (FEM) using ANSYS software and experiment has been performed to verify the developed thermo-mechanical finite element model using Gas Metal Arc Welding (GMAW) process. Also residual stress distribution will investigate only by FEM because experimental process is costly. Our basic aim is to analyse distribution of temperature and residual stresses in welding plate to avoid future failure in material. The residual stress gradient near the fusion zone is higher than in any other location in surrounding area. Because of this stress gradient, cold crack at the fusion zone in high strength steel occur. The main objective of this simulation is the determination of temperatures and stresses during and after the process. Temperature distributions define the heat affected zone where material properties are affected. Simulation process shows that higher residual stress is distributed in weld bead and in Heat Affected Zone (HAZ) Stress calculation is necessary because high residual stresses may be causes fatigue, fractures and stress corrosion such undesirable failures in the regions near weld bead.

Keywords: GMAW, FEM, Thermo-mechanical simulation, distortion, residual stress, heat affected zone, fatigue.

I. INTRODUCTION

ARC welded joint is one of the most important joining methods in manufacturing industry. Accordingly, steel and steel products are the most commonly used products in the welding technique. Material composition and temperature variations in welds and parent metals have important effects on material characteristics, residual stresses, dimensional and shape accuracy of welded fabrications. Arc welding is one of the mostly used fabrication process in the industry due to its applications. During welding process, the thermal stresses are generated in the specimen causing distortion and change in the shape. This problem of residual stresses and distortion of welded plates has become a major issue of research on shipbuilding and machine tool bodies. The goal of thermo mechanical analysis is to realize the significance of simulation of arc welding using finite element method. In machine industry and automotive industry the thin steel metals are used. In them distortion is formed after the arc welding. Due to level of quality of material the failure of material is occurs. So, it is important task to predetermine these problems before welding process is to be done. One method of prediction of welding process is "try and see" method. But this method is time consuming and costly. Therefore there is need of such method which will save time and money in other sense it will give results in short duration. So FEM is usually preferred to monitor and predict the welding process. A. Anca et al. [1] focused on 3D-thermo- mechanical simulation of welding processes. The main objective of this simulation is the determination of temperatures and stresses during and after the process. Temperature distribution define the heat affected zone where material properties are affected. Comparison between analytical and numerical results for a non-isothermal solidification test case were presented. H. Yu et al. [2] investigated temperature distribution of aluminum plates welded by gas tungsten arc. The steady state temperature profile of the welded plates were solved by finite difference method. An increase in the heat input is result in the increasing temperature of welded plates and an increase in welding speed produces opposite effect. L. Yajiang et al. [3] done work on finite element analysis of residual stress in the welding zone of a high strength steel. They found residual stress on goes up to 800-1000 MPa and it is 500-600 below weld. They concluded that residual stress in the direction of width of test plate has highest influence on the formation of cold crack. S. Naser et al. [4] studied the transient variation of thermal stresses and the resulting residual stresses within a thin plate during welding processes. Variation of thermal and residual stresses are investigated inside a thin mild steel plate during welding processes. High residual tensile stresses reaching the yield limit at room temperature are produced close to the weld line after cooling of the plate and residual stress distribution along any transverse section are same except at the edges. It is found that as the weld speed decreases, the temperature inside the plate increases and the residual stresses reaching the yield limit are produced in wider areas along the welded area. M Sundar et al. [5]assessed residual stress and distortion in welding by finite element method. According to them experimental analysis is costly so they prefer FEM analysis. They concluded that transverse residual stresses are high near the weld and reduces as it move further. This is because yield force immediately after welding is very low and part of specimen near the weld deform plastically under very low external load. M. Abid et al. [6] studied the 3-D thermal finite element analysis of single pass girth welded low carbon steel pipe-flange joints. They presented detailed computational procedure for predicting the complete thermal history including transient temperature distribution during girth welding and subsequent post weld cooling of low carbon steel pipe-flange joints. In the analysis, the axial temperature profile at 4 different section on both sides weld joints is presented. The simulated result shows that the temperature distribution around the implemented heat source model is steady when the weld torch moves around the circumferential joint. P Biswas et al. [7] done numerical and experimental study on prediction of thermal history and residual deformation of double sided fillet welding. The temperature distributions obtained from experimental measurements compared fairly well with a variation of only 8

percent for the peak temperatures. The angular distortions obtained through the finite element analysis and those obtained from experimental measurements compared fairly well with variation of 5-10 percent only for the maximum distortions. N Akkus et al. [8] performed thermo mechanical analysis of arc welded joint by finite element method. After comparing simulation results with the experimental results, they found that both the results are nearly same but experimental procedure is costly and time consuming. They concluded that by the usage of the simulation in the welding, errors can be avoided and welding quality can be increased and also simulation can be applied to complex products. This study realizes the simulation of gas metal arc welding. It can be improved in a way that will include not only single pass welding but also multi-pass welding, and may be developed to perform simulation of the welding application in several points in complex products. R. Kovacevic et al. [4] carried out numerical and experimental study of thermally induced residual stress in the hybrid laser- GMA welding process. They use both simulation and experiment process to obtain stress distribution and temperature distribution in the weld. Numerical simulation shows that higher residual stresses is distributed in the weld bead and surrounding heat affected zone. Effect of welding speed on the isotherm and residual stress of the welded joint are also studied. They found that an increase in welding speed can reduce the residual stress concentration in the weld specimen.

II. PROCEDURE

A. Experimental process description

The experiment was carried on a semi-automatic GMAW machine for welding of AISI 202 material using filler wire of AISI 308L. It is 3 phase, 50Hz frequency, 300A current, forced air cooling machine of size 760x313x500mm. The trolley is used to travel work piece which will move at perfect path with speed varying up to 65cm/sec. Gas flow rate in the welding can be adjusted and measure with the help of flow meter. Also, wire feed rate, welding voltage and current are adjusted in the GMAW machine and the speed of the welding can be adjusted and measured. The welded test work piece had the dimensions of 250x100x10 mm. The groove angle between welded pieces is 60^0. The K type thermocouple is used for measuring the temperature distribution in the plate after the welding. The tip diameter of thermocouple is 1.5mm and wire length is 300mm. The thermocouples arrangement on the welding plate for measuring temperature distribution is as shown in fig. (1). The tip of three thermocouple is kept at three different locations on a top surface in a vertical position and temperature is indicated by temperature indicator as shown in fig. (1).

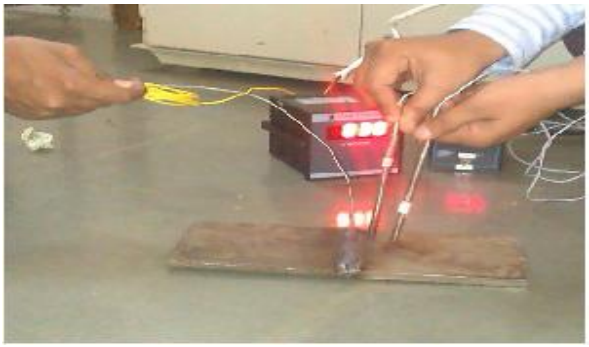

Figure 1. Experimental set up

B. Simulation procedure using ANSYS

The simulation procedure consist of three distinct steps:

- build the model,
- apply loads and obtain the solution,
- review the results.

Figure 2 shows the detailed sequential coupled thermo-mechanical simulation strategy adopted.

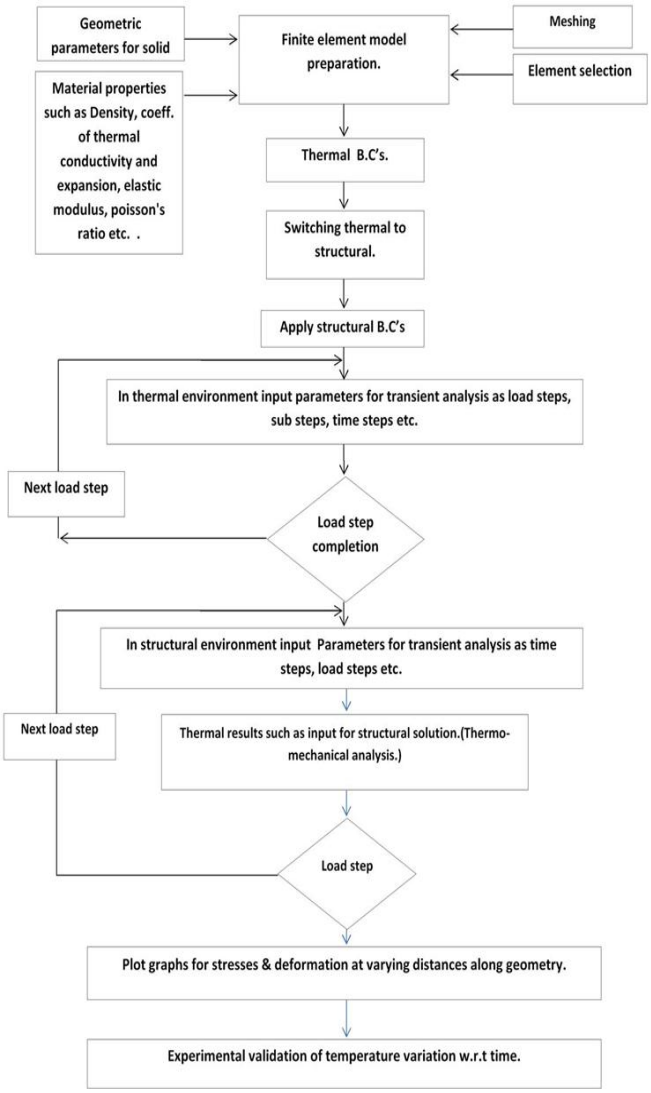

Figure 2. Flowchart of simulation procedure

Table 1: Thermal material properties

Temperatures (^{0}C)	Thermal conductivity (W/m-^{0}C)		Thermal expansion coefficient (x10^{-6}/^{0}C)	
	AISI 202	AISI 308L	AISI 202	AISI 308L
100	16.2	16.1	17.5	17.2
200	17.5	17.3	17.8	17.6
300	19	18.7	18.4	17.8
400	20.8	20.1	18.8	18.1
500	21.6	21.6	19.2	18.4
600	21.9	23.2	19.6	18.8
700	22.2	24.6	19.9	19.1
800	22.6	26.3	20.2	19.6
900	23.2	28.2	20.4	20
1000	23.6	29.5	20.6	20.3
1100	23.9	31.8	20.8	20.6

The welded test work piece has the dimensions of 250x100x10 mm. The groove angle between welded pieces is 60^0. By using dimensions, model is prepared as shown in fig. 3(a).

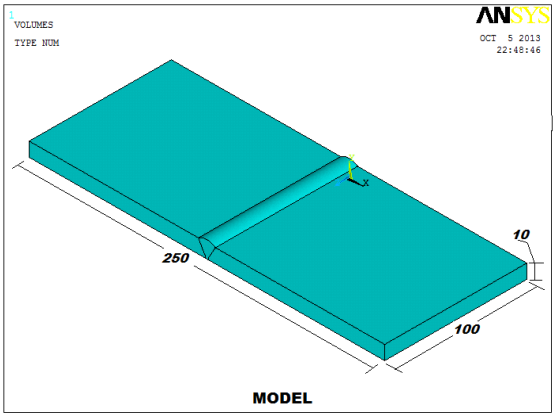

(a) simulation model

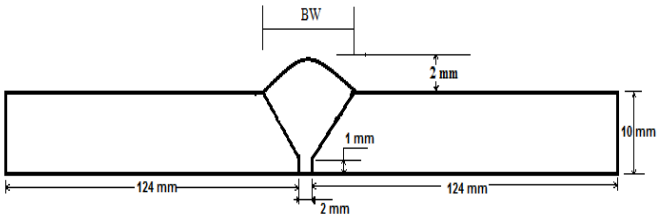

(b) bead geometry

Figure 3. Model developed.

The model with the FE mesh has been shown in Fig.4. The eight- node brick elements with linear shape functions are used in meshing the model. The SOLID70 and SOLID185 elements have been used for meshing. SOLID70 has a three-dimensional thermal conduction capability. The element has eight nodes with a single degree of freedom, temperature, at each node. The element is applicable to a three-dimensional, steady-state or transient thermal analysis. The element also can compensate for mass transport heat flow from a constant velocity field. If the model containing the conducting solid element is also to be analyzed structurally, the element should be replaced by an equivalent structural element (such as SOLID185). Total number of elements after meshing are 5992.

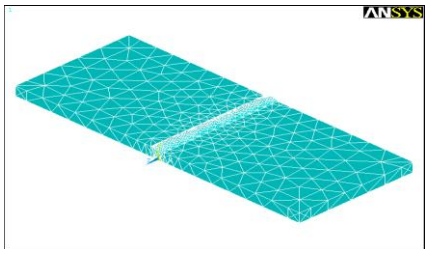

Figure 4. Meshed model

The temperature of 1385^{0}C (melting point temperature of filler material AISI 308L) is given at the welded joint that is between the plates along the centre line. Bulk temperature of 28^{0}C is given at the end of the plates. The simulation has been carried out for thermal analysis in a time period of 1000 seconds. The number of sub steps are 5. The time at the end of load step is 1000 second. The time step size is 200 seconds. The model with thermal boundary conditions has been shown in fig.(5)

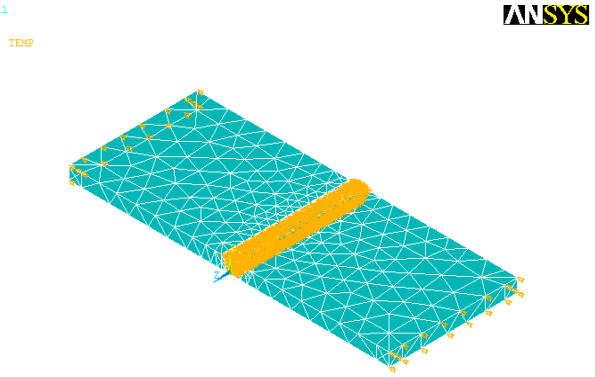

Figure 5. Thermal boundary conditions

Clamping has done at the end surfaces to avoid distortion while welding of plates. As effect of clamping at both end surfaces, vertical displacement of plates due to welding force is constrained. The model with structural boundary condition has been shown in fig.(6)

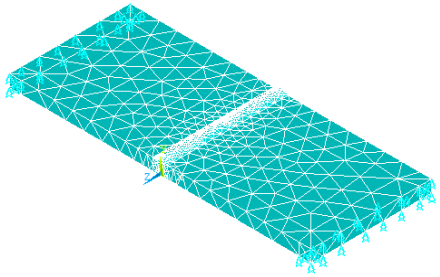

Figure 6. Structural boundary conditions

III. RESULTS AND DISCUSSION

As shown in Fig. 7(a) cross sectional view of weld bead with three points at three different locations (at weld zone, heat affected zone and base metal) at the top surface of the weldment and the distance from the centre line. The temperature distribution curve are plotted at these three locations with respect to time as shown in the fig. 7(b). It is observed that high temperature exist at the weld zone where melting occurs by arc heating. When the welding process is done, welded specimen is cooled up to the room temperature (28^0C) in air. Temperature value decreases when further moving away from the centre line of the weldment. Fig.7 (b) shows that the maximum temperature reaches to 1440^0C at weld zone (at point P3). Similarly at point (P1 and P2) on parent plate maximum temperature values are decreases. Figure 10(a-d). shows the stress distribution along weld bead at three different paths at the top surface of weld bead at z=20, 50 and 80 mm. Figure 10(a) shows that maximum compressive stresses are formed near the weld bead. The intensity of stresses are more at the middle of weldment and nearly same at 20mm and 80mm. The same amount of tensile stresses are induced near end surfaces due to clamping. At z=50mm, compressive residual stresses of about 300 MPa near the weld bead are developed. Fig. 10(b) shows that compressive normal stresses are developed at end surfaces due to clamping. Similarly compressive stresses are more at weld bead and tensile stresses are developed on heat affected zone. Residual stresses of range 50-100 MPa are developed at the weld bead. Fig.10(c) shows that more compressive stresses are induced near the weld bead. Compressive stresses upto 470 MPa are developed at the weld zone. Similarly tensile stresses developed in the parent material zone are about 150 MPa. The little amount of compressive stresses are induced near the end surface of the weldment. The tensile and compressive stresses are maximum at middle of the weldment. Fig. 10(d) shows that all the stresses are tensile in nature and it is maximum at weld bead and minimum at the end of the weldment. Von mises stresses developed at the weld bead are upto 380 MPa. Figure 11(a-d) shows the stress distribution across the weld bead at the middle section (z = 50mm) along thickness. Fig.11(a) shows that residual compressive stresses are maximum near weld bead zone and tensile stresses are observed in base material near the end surfaces. The end portion of the weldment is free from stresses. The residual compressive stress of nearly 300 MPa are developed in the weld zone. Fig. 11(b) shows that compressive stresses are developed at weld bead. Residual compressive stresses of 50-150 MPa are developed at the weld zone. Also little compressive stresses are developed near end surfaces. Stresses induced at all locations are almost same. Fig. 11(c) shows that longitudinal stresses at middle, top and bottom surface are same. More compressive stresses are developed near the weld bead upto 500 MPa. Also tensile stresses induced in parent material. Figure 11(d) shows that all the stresses are tensile in nature and it is maximum at weldment and minimum at the end of the weldment. The tensile stresses are goes on decreasing as move away from weld bead zone. Von mises stress developed in entire weldment is nearly same. From fig 10(a-d) and 11(a-d), it is observed that at weld zone compressive stresses are developed which are more than yield strength of material. Hence failure may occur at the weld zone if maximum loading is done at this zone.

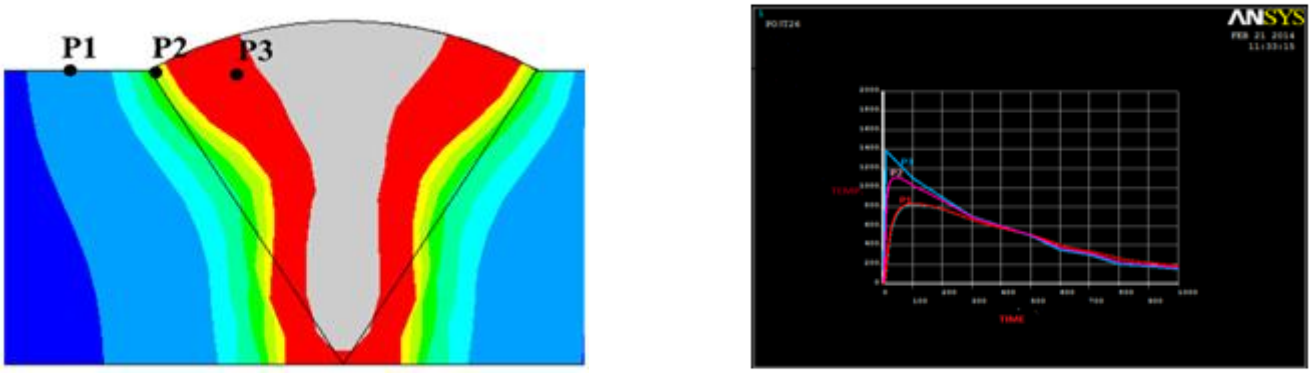

(a) (b)

Figure 7. Temperature distribution at various locations (a) cross sectional view of weld bead, (b) temperature distribution curve

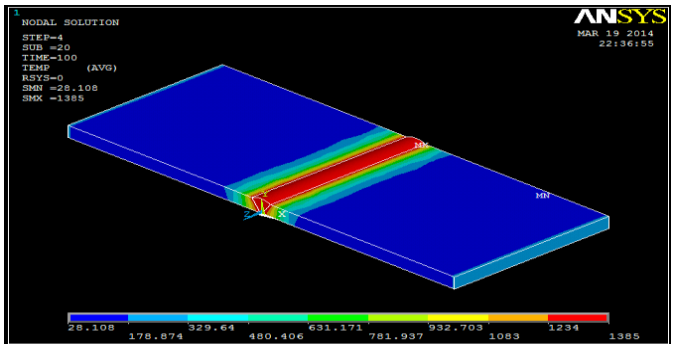

(a)

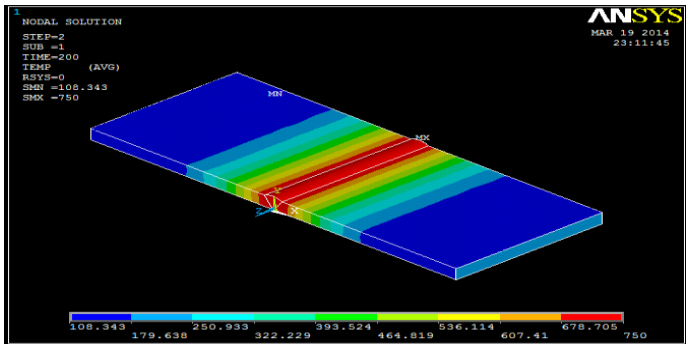

(b)

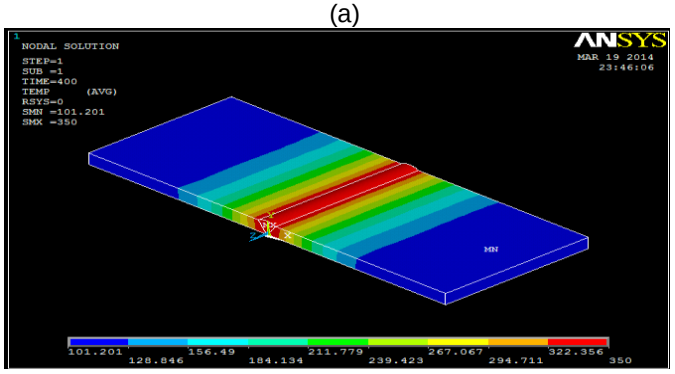

(c)

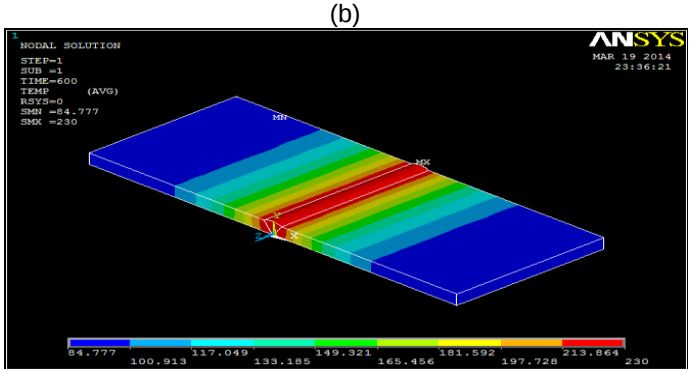

(d)

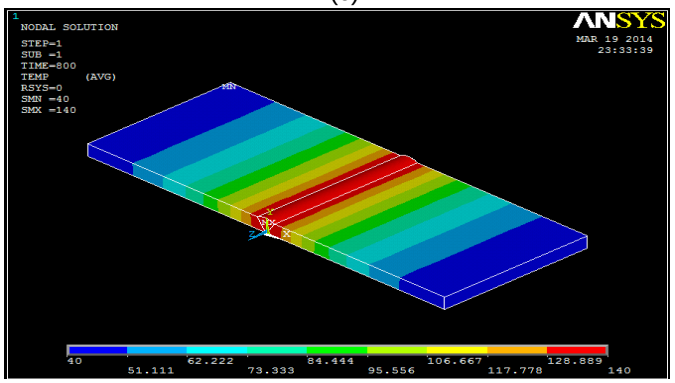

(e)

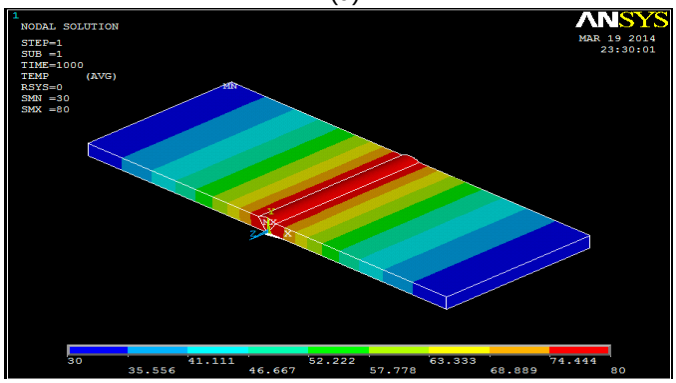

(f)

Figure 8. Temperature distributions along plate due to conduction at different times a) at t=20 sec, b) at t=200 sec, c) at t= 400 sec, d) at t= 600sec, e)at t=800 sec, f)at t=1000 sec.

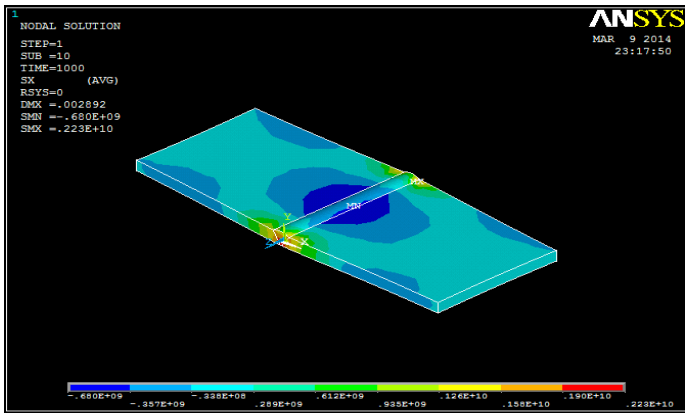

(a)

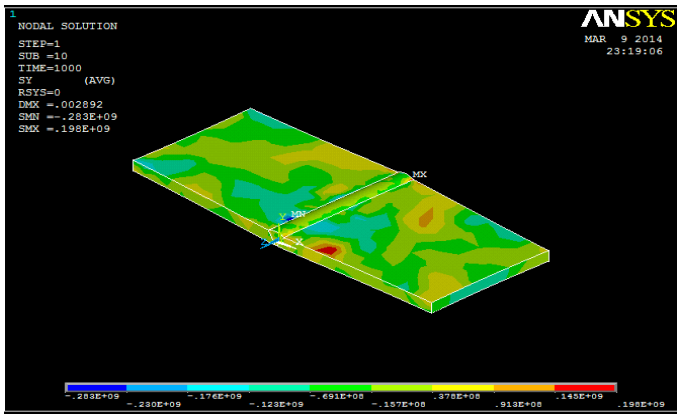

(b)

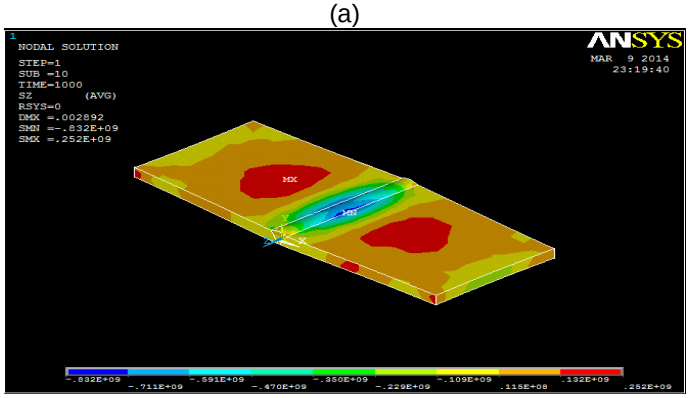

(c)

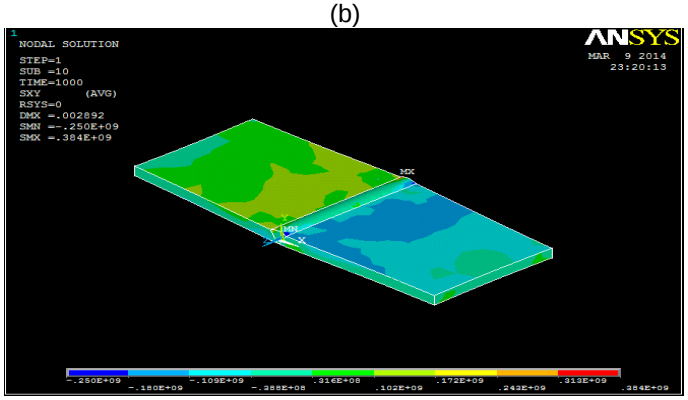

(d)

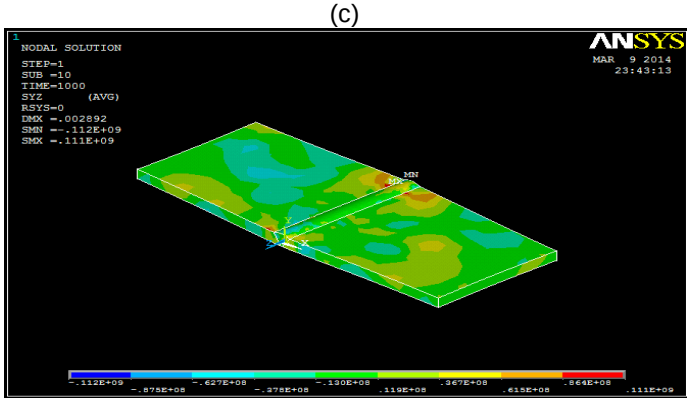

(e)

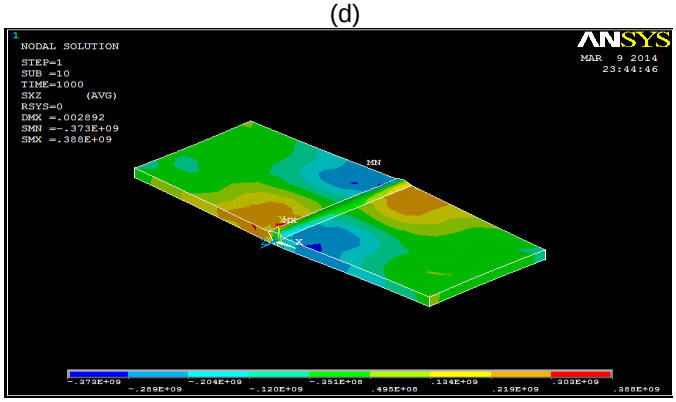

(f)

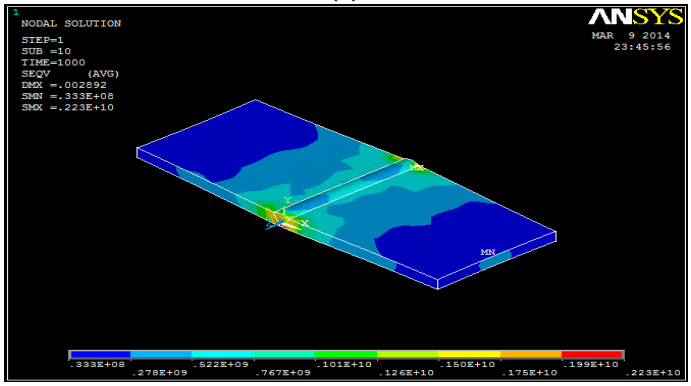

(g)

Figure 9. Residual stress distribution: (a) transverse stress SX, (b) normal stress SY, (c) longitudinal stress SZ, (d) x–y plane shear stress SXY, (e) y–z plane shear stress SYZ, and (f) z–x plane shear stress SZX, (g) Von mises stress SEQV.

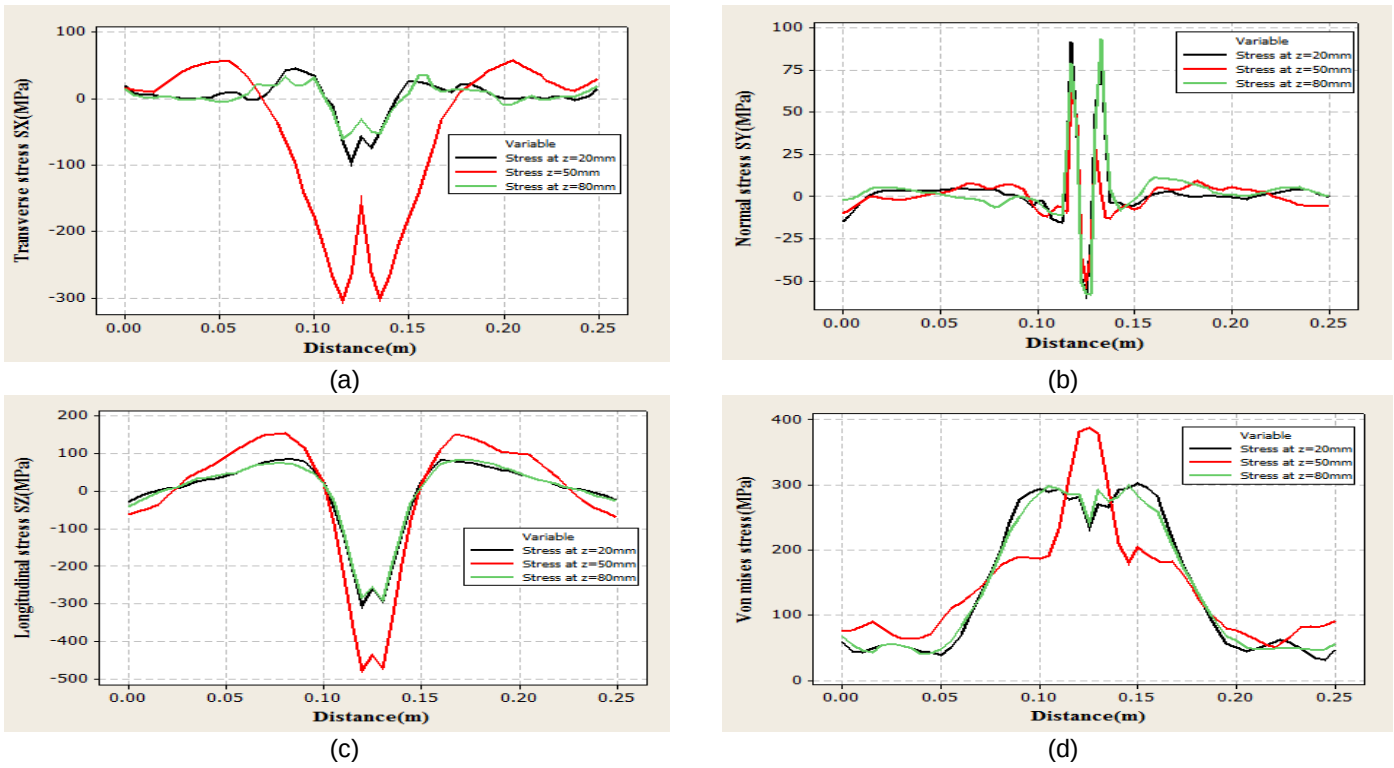

Figure 10. Stress distribution along weld bead at three different paths at the top surface of weld bead obtained by GMA welding: (a) transverse stress SX, (b) normal stress SY, (c) longitudinal stress SZ, and (d) Von Mises stress SEQV.

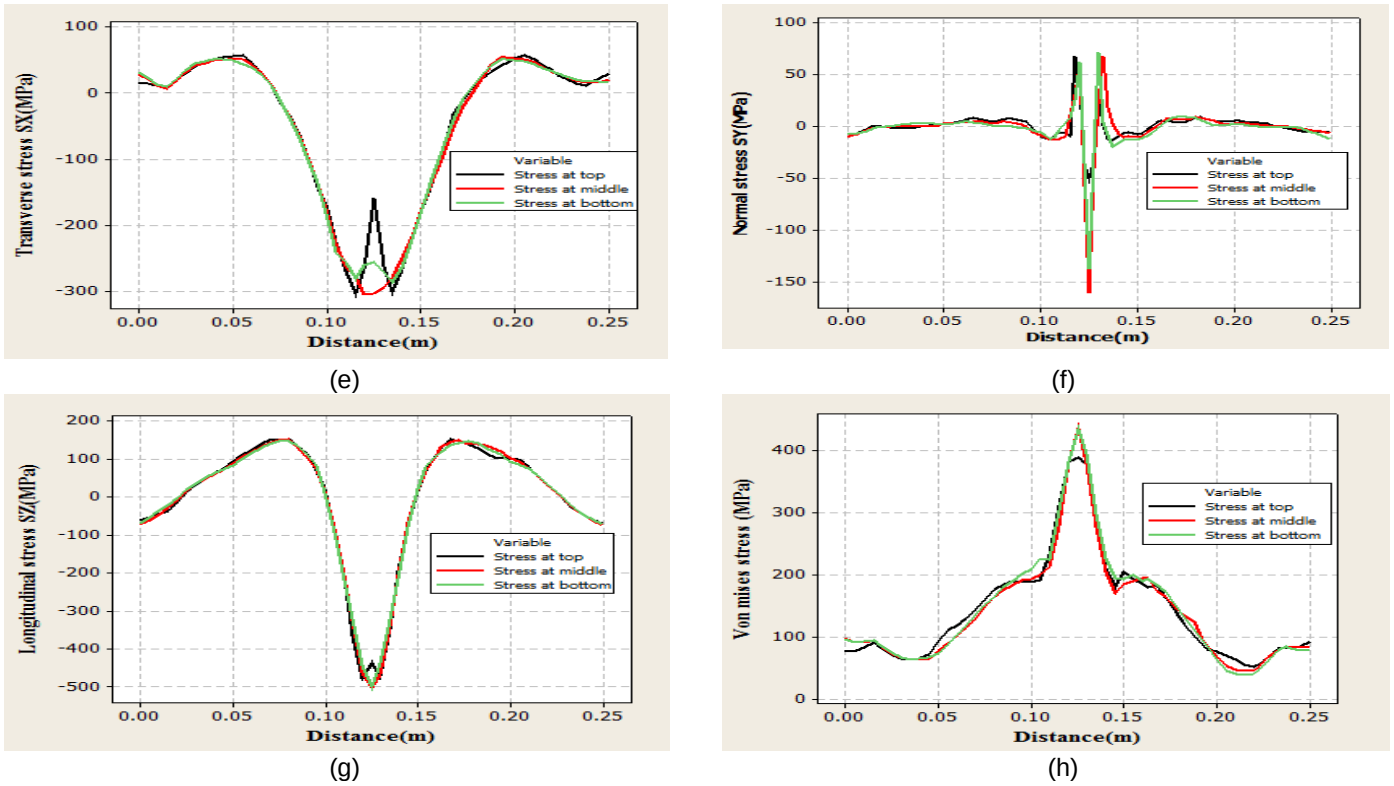

Figure 11. Stress distribution across the weld bead at the middle section (z = 50mm) along thickness: (a) transverse stress SX, (b) normal stress SY, (c) longitudinal stress SZ, and (d) Von mises stress SEQV.

IV. COMPARISON OF SIMULATION AND EXPERIMENT RESULTS

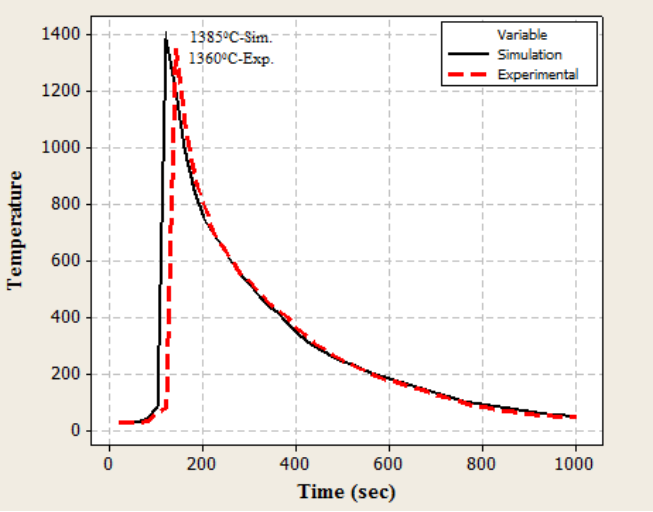

Figure 12. Comparison of simulation and experimental thermal profiles.

Fig. 12 shows the simulation and experimental temperature distribution profiles. The experimental point (thermocouple position) for the thermal history were located at the weld bead on the top surface of horizontal plate. It is observed from figure that there is a close agreement between the simulation and experimental thermal profile. The FEM model predicts a little more temperature than the measured peak temperature. A small temperature gradient difference is due to effect of radiation in experiment. In this study, an experiment was conducted to verify the simulated results. As the simulation thermal profiles are nearly matching with experimental results it can be predict that stress profiles got by simulation must be correct.

V. CONCLUSION

According to results in this study, the following conclusions can be drawn:

1) There is a close agreement between the simulation and experimental thermal profile. As the simulation thermal profiles are nearly matching with experimental results, it can be predict that stress profiles got by simulation must match with experimental profile.

2) There are different experimental methods for measuring residual stresses developed in welded parts such as hole method, X- ray diffraction method etc. But experimental measurements are costly, require equipment and time consuming. However, finite element package is enough for getting results with negligible variation to that of experimental results.

3) Simulation process can be carried out where welding applications deals with complex products.

ACKNOWLEDGMENT

The authors want to thank Prof. A.G. Kamble ,Asst. Professor in Mechanical department, SIT, Lonavala, Pune, for his valuable help in the execution of experiments.

REFERENCES

[1] M Sundar, G Nandi, “Assessment of residual stress and distortion in welding by finite element method”, International conference on mechanical engineering 2005, Dec 2005,Vol. 1, pp. 1-6.

[2] N.Akkus, E. Toptas, “Thermo-mechanical analysis of arc welded joint by finite element method”, AWST, Oct. 2011,Vol. 20, pp. 24-25.

[3] P. Biswas, “Numerical and experimental study on prediction of thermal history and residual deformation of double-sided fillet welding”, J. Engineering Manufacturing, 2009, Vol. 224, pp. 125-134.

[4] Fanrong Kong, Junjie Ma, Radovan Kovacevic, “Numerical and experimental study of thermally induced residual stress in the hybrid laser–GMA welding process”, Journal of material processing technology, USA, Jan 2011,Vol. 123, pp.1102-1111.

[5] Li Yajiang, Wang Juan, “Finite element analysis of residual stress in the welded zone of a high strength steel”, Indian academy of sciences, April 2004, vol. 27 no. 2, pp. 127-132.

[6] S. Naser, “Transient Variations Of Thermal Stresses And The Resulting Residual Stresses Within A Thin Plate During Welding Processes”, Journal of thermal Stresses, Taylor And Francis Group, 2004, Vol. 27, pp. 671-689.

[7] H. Lee, “Numerical And Experimental Investigation Into Effect Of Temperature Field On Sensitization Of AISI 304 in Butt Welds Fabricated by Gas Tungsten Arc Welding”, Materials Transactions, 2011, Vol. 52, No. 7, pp. 1506-1514.

[8] Dr. Hani Aziz Ameen, ”Influence of the butt joint design of TIG welding on the thermal stresses”,eng.& Tech. Journal, 2011,Vol. 400,pp.400-420.

[9] H. Yu, “Thermal Analysis Of Welding On Aluminium Plates”, Journal Of Marine Science And Technology,2003, Vol. 11, No. 4, pp. 213-220.

[10] A. Anca, “3D-Thermal-Mechanical Simulation Of Welding Processes”, MecanicaComputacional, Vol. 23, pp.2301-2318.

[11] Rahib Kamal Kassab, “Experimental and finite element analysis of a T-Joint welding”, Journal of mechanical engineering and automation, 2012, Vol. 400, pp. 411-421.

[12] M. Abid, “3D thermal finite element analysis of single pass girth welded low carbon steel pipe-flange joints”, Turkish J. Eng. Env. Sci., 2009, Vol.33, pp.- 281-293.

[13] Dragistramenkovic, “Finite element of residual stress in butt welding two similar plates”, scientific technical review, Serbia, 2009, Vol. 23, pp.342-360.

[14] M.Kaldhar, K.Venkata, “Optimization of process parameters in turning of AISI 202 austenitic stainless steel”,ARPN journal of engineering and applied science, sept2010, Vol. (5) No. (9), pp.440-450.

[15] Carpinteri, “Fully Three-Dimensional Thermo-Mechanical Analysis Of Steel Welding Processes”, ELSEVIER Journal Of Materials Processing Technology, 1995, Vol. 53, pp. 85-92.

[16] X. Zhu, Y. Chao, “Effects of temperature-dependent material properties on welding simulation*”* Department of Mechanical Engineering, University of South Carolina, Columbia, SC 29208, USA, 11 January 2002, pp. 967–976.